Journal of Applied Physics METHOD pubs.aip.org/aip/jap

Determination of light-independent shunt resistance in CIGS photovoltaic cells using a collection function-based model

Cite as: J. Appl. Phys. **136**, 024502 (2024); doi: 10.1063/5.0216936
Submitted: 2 May 2024 · Accepted: 28 June 2024 ·
Published Online: 10 July 2024

View Online Export Citation CrossMark

M. El Khoury, M. Moret, A. Tiberj, and W. Desrat[a)]

AFFILIATIONS

Laboratoire Charles Coulomb (L2C), Université de Montpellier, CNRS, Montpellier FR-34095, France

[a)]**Author to whom correspondence should be addressed:** wilfried.desrat@umontpellier.fr

ABSTRACT

Shunt resistance R_{sh} is a critical parameter for photovoltaic cells designed for low light indoor applications because it negatively affects the open circuit voltage, fill factor, and conversion efficiency. Standard CIGS cells are known to have low R_{sh} and are, therefore, unpromising candidates for indoor energy sources. In this paper, we extend the original work of Virtuani *et al.* by determining the electrical specifications of many CIGS cells with copper contents [Cu]/([Ga]+[In]) as low as 0.33 and gallium contents between 0.28 and 0.81. First, IV data are fitted by a standard single-diode electrical circuit model for each illumination, resulting in light-dependent parameters. Then, we use a procedure based on a single dataset of electrical variables, i.e., independent of light, corrected by the experimental collection function, which captures light-dependent physical mechanisms. In this way, we are able to correctly reproduce the illuminance dependence of the electrical response of the PV cell over three orders of magnitude, in particular with a fixed value of the shunt resistance. The highest *Rsh* is obtained with a low copper composition of 0.5, regardless of the gallium composition.

I. INTRODUCTION

Cu(In,Ga)Se_2-based photovoltaic (PV) cells are now a mature technology in solar energy conversion.[1–3] Successive improvements over time, such as the three-stage deposition process or the alkali post-deposition treatment, have led to an improved device structure that provides the maximum conversion efficiency for the AM1.5 solar spectrum. In these cells, the CIGS absorber is close to stoichiometry with a ratio [Cu]/([Ga]+[In]) ∼ 0.9 and an average gallium content of [Ga]/([Ga]+[In]) ∼ 0.35.

The potential of CIGS photovoltaic cells for indoor applications has been poorly studied in the past, mainly because standard structures optimized for outdoor conditions have low shunt resistances. Indeed, the uneven CdS/CIGS interface and the presence of pinholes and grain boundaries in the absorber tend to favor shunting pathways.[4] The strong contribution of current shunting the diode dominates under low light conditions and is detrimental to the open circuit voltage, which then decreases proportionally to the photocurrent. Indoor illuminance is generally less than 1000 lx, while outdoor illuminance is of the order of 100 klx. As a consequence, standard CIGS cells at low illuminances are characterized by extremely low open circuit voltages, low fill factors, low conversion efficiencies, and, thus, negligible electrical powers. Virtuani *et al.*[5–7] demonstrated that the shunt resistance can be significantly increased by reducing the copper content in the absorber alloy, while the thickness of the ZnO:Al and CdS layers does not play a role in the improvement. The authors focused on CIGS cells with a [Ga]/([Ga]+[In]) ratio, hereafter referred to as *GGI*, of 0.33. The *CGI* ratio, i.e., [Cu]/([Ga]+[In]), was between 0.59 and 0.89.

In the present work, the earlier study is expanded to investigate the electrical properties of CIGS thin films on wide copper and gallium composition windows, with $0.33 < CGI < 1$ and $0.28 < GGI < 0.81$. The IV characteristics of all cells are measured as a function of the illuminance of a white LED over a range of three orders of magnitude. This complete dataset allows extraction of the light-dependent electrical specifications of components that make up the single-diode PV cell model at each alloy composition. In the second step, we consider the light-independent parameters, complemented by the collection function that includes

all light-dependent physical mechanisms.[8–11] Our main result is the drastic increase in shunt resistance by more than two orders of magnitude with the reduction of copper to $CGI = 0.45-0.5$, where *Rsh* is maximum, $\sim 100\,\mathrm{k\Omega\,cm^2}$, independent of the *GGI* ratio. It increases the open circuit voltage and results in a one thousand times higher maximum power compared to copper stoichiometric CIGS cells at very low illuminances.

II. CELL FABRICATION AND MEASUREMENTS

The photovoltaic cells studied are the standard ZnO/CdS/CIGS/Mo heterostructures grown on soda-lime glass substrates. First, molybdenum back contact is deposited by RF sputtering, following the technique optimized by Briot *et al.*[12] The CIGS absorber layer is grown on top by co-evaporation of pure copper, indium, gallium, and selenium. The deposition is performed in a single step run of 80 min with a constant atomic flux of all chemical species throughout the process. This step results in a $2\,\mu$m thick CIGS film for a standard cell. The n-type CdS layer is deposited in an ammonia solution consisting of thiourea and cadmium sulfate, and i-ZnO and Al-ZnO top windows are obtained by RF sputtering from *ad hoc* targets. Three batches of cells were grown, each defined by an almost constant gallium content, but different copper compositions in each series. The target values of the *GGI* ratio were 0.28, 0.64, and 0.81. The *CGI* ratio was reduced from ~1 for high copper alloys to 0.4 for low copper materials. The alloy compositions were tuned by acting on the relative rate of the partial pressures of precursor beams during growth, allowed by a precise control of the temperature of the effusion cells. The growth of the absorber by a single-step protocol results in a layer with a relatively homogeneous alloy composition along the growth axis, in contrast to the composition gradient that occurs in three-step CIGS cells. The single-step approach, in which all elements are evaporated simultaneously, also makes it easier to control the chemical composition from high to low copper and/or gallium content. It would have been difficult to produce similar gallium gradients on such a large copper content scale. The compositions of all samples were measured by energy dispersive x-ray spectroscopy (EDS) by averaging over a sufficiently large rectangular area ($100 \times 100\,\mu\mathrm{m^2}$). The *GGI* and the *CGI* ratio given below are the measured values. Electrical specifications were obtained on $0.5 \times 0.5\,\mathrm{cm^2}$ square cells, realized by mechanical scribing, with an indium top contact at the center. The current vs voltage (IV) measurements were systematically performed on about 20 cells for each batch, and light dependence was performed on the best cell at the arbitrary illuminance of 1000 lx, a standard value for indoor investigations.[13] Raw values are plotted directly in the following graphs and are not scaled per unit area. The current vs voltage (IV) characteristics are measured with a Keithley 2401 sourcemeter at a fixed illuminance provided by a white LED. The illuminance dependence is performed by varying the LED supply current to cover nearly three orders of magnitude, from 50 lx to 60 klx. The white LED is a 5000 K Bridgelux BXRE-50S and the illuminance is calibrated with a C.A 1110 Chauvin Arnoux luxmeter.

III. FITTING IV CURVES WITH LIGHT-DEPENDENT ELECTRICAL PARAMETERS

The illuminance dependence of the IV curves measured in $GGI = 0.81$ and $CGI = 0.99$ cells is shown in Fig. 1, where the absolute value of the current is plotted. The vertical axis is on a logarithmic scale, allowing observation of three orders of magnitude of the photogenerated current from $1\,\mu$A to ~1 mA at $V = 0$ V, indicated by the vertical line. The horizontal axis is linear because the open circuit voltage decreases gradually from 0.55 V to 0. Each IV curve is fitted with a classical single-diode electrical model consisting of a series resistance *Rs* and a shunt resistance *Rsh* in parallel with a diode, characterized by its saturation current I_0 and its ideality factor *n*. The fits are performed over a wide voltage range, from $V = -0.3$ V to 0.8 V, in order to accurately estimate both resistances *Rsh* and *Rs*, as shown by the good agreement of the solid lines in Fig. 1. This large fitting window is even more indispensable at very low illuminances, when the photocurrent generating operation of the cell is greatly reduced for negligible positive voltages between zero and a very weak open-circuit voltage, *Voc*.

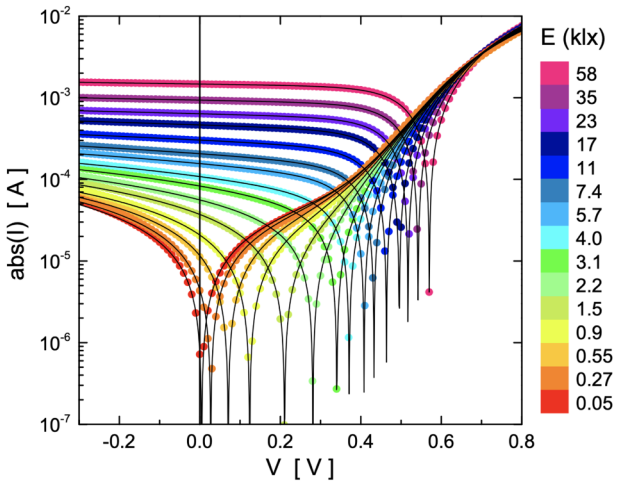

FIG. 1. Current–voltage characteristics measured in a CIGS cell with $GGI = 0.81$ and $CGI = 0.99$ as a function of the illuminance of a white LED in the range of 50 lx–60 klx. The dots are the experimental data and the solid lines are the fits by the single-diode model.

Various parameters of the DC electrical circuit are plotted as a function of LED illuminance, *E*, in Figs. 2(a)–2(d), for three CIGS cells with different copper and gallium contents. These three cells were chosen for their very different values of shunt resistance [see Fig. 2(d)], ranging from a few 100 Ω to several kΩ. It is worth noting that there is no general trend for the light dependence of each parameter. For example, the reverse current and the ideality factor of the diode start to decrease when the illuminance is reduced from high intensities, but then, they can saturate (dot and triangle series) or even increase again (square series) at low light levels. The illuminance dependence of series resistance is also ambiguous, with a monotonic increase, a bell-shaped curve, or a quasi-constant value observed for different cases. The shunt resistance in Fig. 2(d) tends to increase and then saturate as the light intensity decreases for all cells, but the amplitude of the R_{sh} variation differs from sample to sample. In fact, the ratio of the dark shunt resistance to that extracted

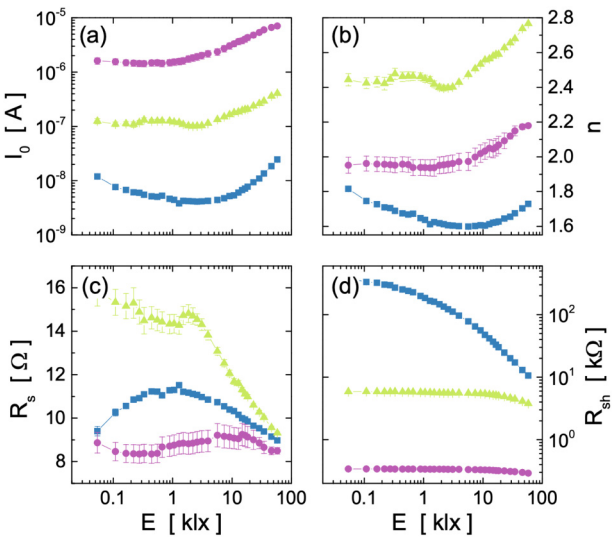

FIG. 2. (a)–(d) Fitting parameters of the single-diode electrical model, *I*0, *n*, *Rs*, and *Rsh*, respectively, vs illuminance. The data of three CIGS cells are plotted with the following compositions: *GGI* = 0.28, *CGI* = 0.94 (purple dots); *GGI* = 0.81, *CGI* = 0.99 (green triangles); and *GGI* = 0.28, *CGI* = 0.47 (blue squares). Error bars indicate the standard deviation of fit parameters.

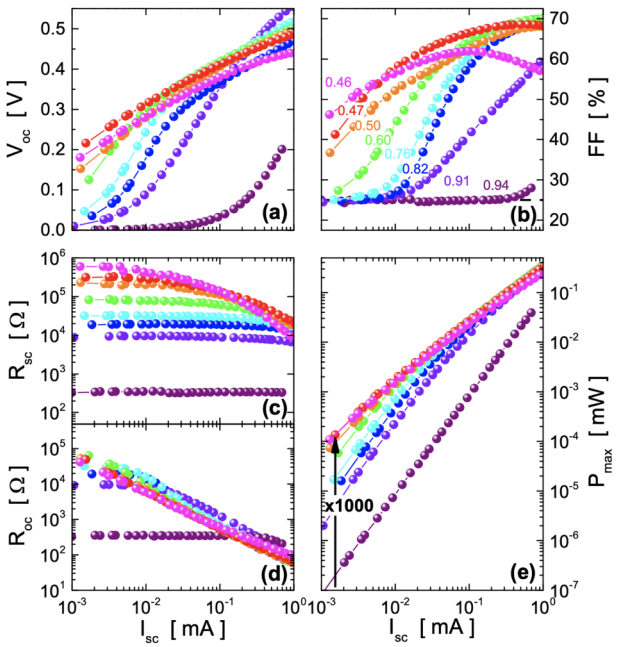

FIG. 3. (a)–(e) Open circuit voltage, fill factor, short circuit resistance, open circuit resistance, and maximum power as a function of the short circuit current for eight photovoltaic cells. The CIGS absorbers have an average *GGI* ratio of 0.28 and *CGI* ratios in the range 0.46 – 0.94, which are indicated in (b).

under 60 klx is equal to 1.2 and 1.5 for the two samples with the lowest R_{sh} but is greater than 35 for the device with the highest resistance. These different behaviors of parameters vs E cannot be attributed to the limit of validity of the electrical model for certain samples or the fitting procedure since all experimental data were fitted identically with equal agreement. The error bars in Fig. 2 show that error propagation, which varies as a function of illuminance or from one sample to another, remains negligible with respect to the variation in the parameters. Thus, the observed variations in electrical characteristics as a function of light intensity appear to be sample-dependent. The lack of consensus on the electrical behavior of CIGS cells vs illuminance is also found in the literature.[5,6,14,15] This will be discussed in Sec. V.

IV. FITTING IV CURVES WITH THE COLLECTION FUNCTION

To get rid of the light dependence of the electrical parameters, we propose to model the DC electrical response of thin film cells in a different way. Instead of fitting all the IV curves measured for each illuminance separately, we first extract the main characteristics from the IV curves, which we then fit as a function of illuminance as a whole. To do this, we measure the short-circuit current *Isc*, the open-circuit voltage *Voc*, the maximum power *Pmax*, the fill factor $FF = Pmax/(Voc \times Isc)$, and the inverse of the IV slopes at the short-circuit and open-circuit operating points, labeled *Rsc* and *Roc*, respectively. These values are extracted directly from the IV curves without any prior assumptions. Figures 3(a)–3(e) show the dependencies of five of these parameters as a function of *Isc* for eight CIGS cells with a common *GGI* ratio of 0.28 and different *CGI* values indicated in the subplot (b). In short, we observe that the open-circuit voltage drops sharply with *Isc* and cancels out for the copper-rich cells (purple-blue curves). It remains above 0.2 V for the lowest *CGI* cell at 50 lx, i.e., $I_{sc} \sim 1\,\mu$A (orange-red curves). The fill factor also increases from 25% for *CGI* = 0.94 to 50%–60% for *CGI* = 0.46 over the full illumination range. Figures 3(c) and 3(d) present a strong increase in *Rsc* and *Roc*, respectively, at low illuminance of more than three orders of magnitude as the copper content decreases. The short-circuit resistance jumps from 300 Ω at *CGI* = 0.94 to 600 kΩ at *CGI* = 0.46. All of these effects lead to a drastic enhancement of *Pmax*, with a factor of 1000 increase at 50 lux between the copper-rich and copper-poor cells, as indicated by the vertical up arrow in subplot (d) of Fig. 3.

To fit these data, we now assume that the four parameters of the basic electrical circuit, namely, *I*0, *n*, *Rs*, and *Rsh*, are independent of illuminance and that all light-dependent physical mechanisms are integrated into an additional term, which is the classical collection function. This contribution, which is ignored in the single-diode electrical model previously used to fit the IV curves (solid lines in Fig. 1), has been intensively studied in the past.[8,9] It is represented either as a subtractive term describing the recombination current[10] or as the fraction of the photogenerated current that is actually extracted from the cell. Many theoretical expressions of the voltage dependence of the collection function are reported in the literature,[11,16] but here, we decide to use the experimental data directly.

For this purpose, the IV curves measured at different illuminances (46, 35, 23.5, 11.8, and 5.8 klx) were used to calculate the normalized collection function, $\eta(V) = (I_1(V) - I_2(V))/(I_{1sc} - I_{2sc})$, where index 1 corresponds to the highest illuminance and index 2 to the lowest illuminance. The collection functions of the three same samples presented in Fig. 2 are plotted in Fig. 4(a), where different symbols are used for the different illuminances. The superposition of the data demonstrates that a single experimental collection function η allows to take into account all light-dependent mechanisms independent of the light intensity. By adding the collection function to the single-diode electrical model, the voltage dependence of the current of the photovoltaic cell is written as follows:

$$I = \eta(V) I\,ph - I0\left[\exp\left(\frac{q(V + RsI)}{nk_BT}\right) - 1\right] - \frac{V + RsI}{Rsh}. \quad (1)$$

Computing this equation for many photogenerated current values allows the IV characteristics to be simulated at any illumination level. Figures 4(b)–4(e) show the experimental points (blue dots) and their respective fits (red solid lines), which show a very good agreement for all measured data over almost three orders of magnitude of illuminance with a single data set of electrical parameters ($I0$, n, Rs, and Rsh) for each sample. We observe that when the shunt resistance is small and bypasses the diode (top row of Fig. 4), the current flows primarily through it. This resistance regime leads to linear IV curves, and Voc is proportional to Isc, as illustrated by the gray dashed curve (the logarithmic scale for Isc makes the linear dependence look exponential). The slopes of the linear IV curves at the short-circuit and open-circuit points are obviously equal, hence the constants Rsc and Roc in subplot (d). The fill factor equals 25% since both current and voltage at the maximum power are half of Isc and Voc. For an intermediate shunt resistance value (middle row in Fig. 4), the contribution of the diode increases so that the open-circuit voltage depends on the logarithm of Isc, i.e., $Voc \approx \frac{nk_BT}{q}\log(Isc/I0)$. At low light levels, the IV curves are still linear and $Voc \propto Isc$. This competition between the shunt resistance and the diode leads to two regimes at low and high illuminances, which are clearly visible for the $GGI = 0.81$ and $CGI = 0.99$ cells. This is accompanied by a decrease in Rsc and Roc toward the series resistance Rs at high illuminance.[10,17] Also, the nonlinear IV characteristics cause the fill factor to become much higher than 25%. Finally, when the shunt resistance is greater than several hundred kΩ, the internal current is negligible and the PV cell is reduced to a diode. In this regime, the open-circuit voltage decreases as $\log(Isc)$[18] and the open-circuit resistance is almost equal to Rs (last row of graphs in Fig. 4). It is interesting to evaluate the influence of the collection function on the illuminance dependence of the short-circuit resistance. By neglecting this term, Rsc remains constant over the whole Isc range [purple dashed line in Fig. 4(d)], while the model including the experimental collection function fits the Rsc data perfectly. It also suggests that when the IV curves are fitted individually without the collection function, as in Sec. III, the effects are partially transferred to the illuminance dependence of Rsh.

V. DISCUSSION

Figure 5(a) displays the shunt resistance for the three GGI batches with different CGI values. It is evident that reducing the

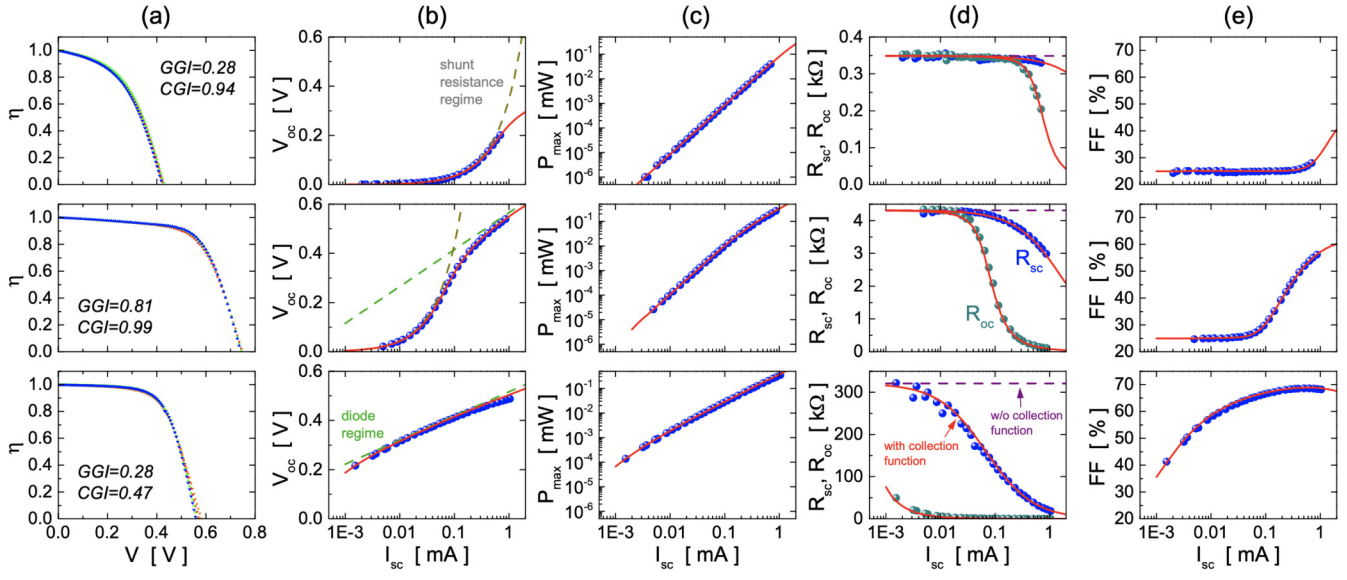

FIG. 4. The experimental collection function [column (a)], open-circuit voltage (b), maximum power (c), short-circuit and open-circuit resistances (d), and fill factor (e) are plotted vs the short circuit current for three different cells (one per row). The GGI and CGI ratios are given in subplots (a). Red solid lines in graphs (b)–(e) result from fits by the equivalent dc electrical circuit model improved by the experimental collection function, plotted in (a). Dashed lines in Voc graphs show the shunt resistance and diode contributions. The horizontal dashed lines in Rsc graphs are the constant slopes vs $I\,ph$ when the collection function is neglected.

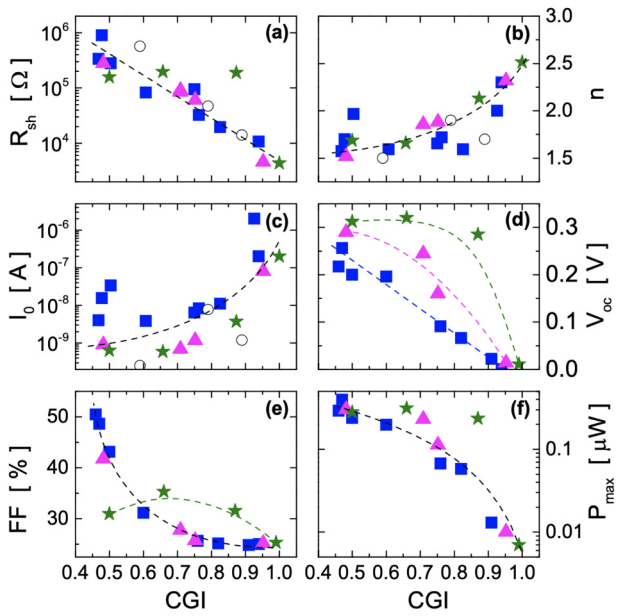

FIG. 5. Fitting parameters from the illuminance dependence of the IV curves vs the *CGI* ratio for the three cell series with *GGI* ratios equal to 0.28, 0.64, and 0.81 (square, triangle, and star symbols, respectively) : (a) *Rsh*, (b) n, and (c) *I*0. Open circles are from Ref. 5. The open circuit voltage (d), fill factor (e), and maximum power (f) measured for an illuminance of 100 lx. Dashed lines are guides for the eyes.

copper content in the CIGS layer from $CGI = 1$ to 0.5 leads to an exponential increase in *Rsh* up to several hundred kΩ. The dependence of the shunt resistance on copper can be approximated by $Rsh \approx 4 \times 10^7 \exp(-9\,CGI)$.[7] We emphasize that the cells fabricated with lower *CGI* ratios of $0.3 - 0.4$ were all short-circuited, preventing the evaluation of the electrical parameters at such low copper compositions. This suggests that a *CGI* of 0.5 is the optimum for the highest *Rsh* in single-stage CIGS thin films. The diode parameters *n* and *I*0 plotted in Figs. 5(b) and 5(c) decrease slightly with decreasing copper composition against all odds. Indeed, this could indicate a better p–n junction and a reduction in the recombination centers with the increasing number of copper vacancies, which is highly unlikely. However, the reduction in the copper content leads to the formation of ordered vacancy compounds (OVC), which cause such significant changes in the absorber layer (doping concentration, defects, crystalline quality, bandgap, and offset) that it is difficult to model their impact on diode specifications. The absence of a gradient in our cells probably has a negative impact on their performance but would not have prevented the formation of very defective OVC layers for CGIs as low as 0.5. Finally, we observe that the data measured in the dark by Virtuani *et al.*[6] [open circles in Figs. 5(a)–5(c)] are in good agreement with our results, but the wider range of *CGI* in our study allows the observation of general trends that were not clearly identified before. It would be tempting to define threshold values for the various parameters of the CIGS absorber guaranteeing good indoor performance, such as a minimum shunt resistance of 10^5 ohms. However, competition between the shunt resistor and the diode in the single-diode model shows that such a criterion would no longer be valid, in the case of a very bad diode.

To illustrate the beneficial influence of a high shunt resistance on the IV curves at very low illuminance, we have plotted the *Voc*, *FF*, and *Pmax* values measured under 100 lx white LED illumination in Figs. 5(d)–5(f). The open circuit voltage takes advantage of the higher *Rsh* with a value of 0.25–0.3 V at 100 lx for all gallium compositions, while it is insignificant for copper-rich cells. The fill factor also doubles passing from 25% to 50% for the $GGI = 0.28$ and 0.64 series. As a consequence, the maximum power under 100 lx is obtained for the *CGI* range from 0.45 to 0.5, whatever the *GGI* ratio, with a value of $\sim 1.5\,\mu W/cm^2$. Note that the $CGI = 0.94$ data shown in Fig. 3 (purple dots) with a shunt resistance of 350 Ω and a maximum power of $1.5\,nW/cm^2$ are not shown in Figs. 5(a) and 5(f) to maintain a reasonable scale. However, considering these data, when the copper content in the CIGS absorber is reduced from 1 to 0.5, the shunt resistance and the maximum power at low illuminance are increased by three orders of magnitude.

We now discuss the differences between our two approaches. It is evident that our second original fitting method allows the extraction of single electrical parameters that are valid over a wide range of illuminances, assuming that the collection function includes all light-dependent physical mechanisms that occur in the cell. The advantage of this method is that individual characteristics can be easily compared between the PV devices. On the other hand, the standard fitting of the IV curves vs illuminance by the single-diode model results in light-dependent parameters that are also sample dependent. In this case, the comparison of the parameters is more difficult. In Fig. 2, two different devices may have similar values at one illuminance but different values at another illuminance. The previous reports on the light dependence of the electrical parameters in CIGS thin films, obtained from the single IV curve fitting method, also lead to controversial light dependence of the electrical parameters.[5,6,14,15] For example, Virtuani *et al.*[6] reported an increase in the shunt resistance from 1.9 kΩ cm^2 under 1 sun to 142 kΩ cm^2 in the dark as well as an increase in the series resistance, which was attributed to the photoconductivity effect in the absorber. At the same time, the *I*0 and *n* parameters were shown not to vary significantly from 0.1 to $100\,mW/cm^2$.[5] Similarly, Bronzoni *et al.* reported that *I*0, *n*, and *Rs* do not change much as a function of light conditions,[14] but *Rsh* increases inversely proportional to irradiance in the range of $30–130\,mW/cm^2$. More recently, the work of Ramesh *et al.* concludes that the shunt resistance and reverse current increase as a power law of decreasing irradiance in the range of $100–1200\,W/m^2$, with an empirical coefficient between −1 and −0.4 for *Rsh* and −0.24 and −0.13 for *I*0.[15] The series resistance does not vary. In conclusion, we see that the variation in the electrical quantities *I*0, *n*, and *Rs* as a function of the light level is often weak, whereas a common trend is observed for the shunt resistance, which reveals a significant increase when the illuminance is lower. This is consistent with our data in Fig. 2(d), where the light dependence is embodied by *Rsh*, or in Fig. 4 where the light-independent shunt value is compensated by the collection function.

VI. CONCLUSION

We demonstrate that the shunt resistance of CIGS photovoltaic cells increases exponentially as the copper composition of the alloy, *CGI* =[Cu]/([Ga]+[In]), decreases from 1 to 0.45, regardless of the gallium ratio between 0.28 and 0.81. This result is obtained by means of an unusual fitting procedure based on a light-independent electrical model of the cell, coupled with the collection function, which allows a perfect agreement of the illumination dependence of the IV characteristics over three orders of magnitude. Our work suggests that a CIGS absorber with a *CGI* ratio of 0.5 is electrically optimal for single-step $Cu(In,Ga)Se_2$-based indoor PV cells.

ACKNOWLEDGMENTS

This paper was financially supported by the Région Occitanie and Programme d'Investissement d'Avenir (PIA3), Campus des Métiers et des Qualifications "Habitat, énergies renouvelables et éco-construction."

AUTHOR DECLARATIONS

Conflict of Interest

The authors have no conflicts to disclose.

Author Contributions

M. El Khoury: Data curation (equal); Formal analysis (lead); Investigation (equal). **M. Moret:** Data curation (equal); Investigation (equal). **A. Tiberj:** Conceptualization (lead); Supervision (equal). **W. Desrat:** Project administration (lead); Supervision (equal); Writing – original draft (lead); Writing – review & editing (lead).

DATA AVAILABILITY

The data that support the findings of this study are available from the corresponding author upon reasonable request.

REFERENCES

[1]K. W. Böer, *Handbook of the Physics of Thin-Film Solar Cells* (Springer Berlin, Heidelberg, 2013).
[2]J. Ramanujam and U. P. Singh, "Copper indium gallium selenide based solar cells—A review," Energy Environ. Sci. **10**, 1306–1319 (2017).
[3]N. Mufti, T. Amrillah, A. Taufiq, Sunaryono, Aripriharta, M. Diantoro, Zulhadjri, and H. Nur, "Review of CIGS-based solar cells manufacturing by structural engineering," Sol. Energy **207**, 1146–1157 (2020).
[4]B. L. Williams, S. Smit, B. J. Kniknie, K. J. Bakker, W. Keuning, W. M. M. Kessels, R. E. I. Schropp, and M. Creatore, "Identifying parasitic current pathways in CIGS solar cells by modelling dark J-V response," Prog. Photovoltaics Res. Appl. **23**, 1516–1525 (2015).
[5]A. Virtuani, E. Lotter, and M. Powalla, "Performance of $Cu(In,Ga)Se_2$ solar cells under low irradiance," Thin Solid Films **431-432**, 443–447 (2003).
[6]A. Virtuani, E. Lotter, M. Powalla, U. Rau, and J. H. Werner, "Highly resistive $Cu(In,Ga)Se_2$ absorbers for improved low-irradiance performance of thin-film solar cells," Thin Solid Films **451-452**, 160–165 (2004).
[7]A. Virtuani, E. Lotter, M. Powalla, U. Rau, J. H. Werner, and M. Acciarri, "Influence of Cu content on electronic transport and shunting behavior of Cu $(In,Ga)Se_2$ solar cells," J. Appl. Phys. **99**, 014906 (2006).
[8]S. S. Hegedus, "Current-voltage analysis of a-Si and a-SiGe solar cells including voltage-dependent photocurrent collection," Prog. Photovoltaics Res. Appl. **5**, 151–168 (1997).
[9]C.-Y. Huang, W.-C. Lee, and A. Lin, "A flatter gallium profile for high-efficiency $Cu(In,Ga)(Se,S)_2$ solar cell and improved robustness against sulfur-gradient variation," J. Appl. Phys. **120**, 094502 (2016).
[10]J. Merten, J. M. Asensi, C. Voz, A. V. Shah, R. Platz, and J. Andreu, "Improved equivalent circuit and analytical model for amorphous silicon solar cells and modules," IEEE Trans. Electron Devices **45**, 423–429 (1998).
[11]S. Hegedus, D. Desai, and C. Thompson, "Voltage dependent photocurrent collection in CdTe/CdS solar cells," Prog. Photovoltaics Res. Appl. **15**, 587–602 (2007).
[12]O. Briot, M. Moret, C. Barbier, A. Tiberj, H. Peyre, A. Sagna, and S. Contreras, "Optimization of the properties of the molybdenum back contact deposited by radiofrequency sputtering for $Cu(In_{1-x}Ga_x)Se_2$ solar cells," Sol. Energy Mater. Sol. Cells **174**, 418–422 (2018).
[13]X. Hou, Y. Wang, H. K. H. Lee, R. Datt, N. Uslar Miano, D. Yan, M. Li, F. Zhu, B. Hou, W. C. Tsoi, and Z. Li, "Indoor application of emerging photovoltaics—progress, challenges and perspectives," J. Mater. Chem. A **8**, 21503–21525 (2020).
[14]M. Bronzoni, L. Colace, A. De Iacovo, A. Laudani, G. M. Lozito, V. Lucaferri, M. Radicioni, and S. Rampino, "Equivalent circuit model for Cu(In,Ga)Se2 solar cells operating at different temperatures and irradiance," Electronics **7**, 324 (2018).
[15]S. Ramesh, A. Tuomiranta, A. Hajjiah, M. Meuris, B. Vermang, and J. Poortmans, "Physics-based electrical modelling of cigs thin-film photovoltaic modules for system-level energy yield simulations," npj Flexible Electron. **6**, 87 (2022).
[16]X. Sun, T. Silverman, R. Garris, C. Deline, and M. A. Alam, "An illumination- and temperature-dependent analytical model for copper indium gallium diselenide (CIGS) solar cells," IEEE J. Photovoltaics **6**, 1298–1307 (2016).
[17]J. Merten, C. Voz, A. Muñoz, J. M. Asensi, and J. Andreu, "The role of the buffer layer in the light of a new equivalent circuit for amorphous silicon solar cells," Sol. Energy Mater. Sol. Cells **57**, 153–165 (1999).
[18]N. H. Reich, W. G. J. H. M. van Sark, E. A. Alsema, R. W. Lof, R. E. I. Schropp, W. C. Sinke, and W. C. Turkenburg, "Crystalline silicon cell performance at low light intensities," Sol. Energy Mater. Sol. Cells **93**, 1471–1481 (2009).